Proceedings of the 2004 IEEE
International Conference on Robotics & Automation
New Orleans, LA • April 2004

A Hop towards Running Humanoid Biped

Shuuji Kajita*, Takashi Nagasaki†, Kenji Kaneko*, Kazuhito Yokoi* and Kazuo Tanie*†
*National Institute of Advanced Industrial Science and Technology(AIST)
Tsukuba, Ibaraki 305-8568, Japan, Email: s.kajita@aist.go.jp
†University of Tsukuba, Email: t-nagasaki@aist.go.jp

Abstract— **Aiming for a humanoid robot of the next generation, we have been developing a biped which can jump and run. This paper introduces biped robot HRP-2LR and its hopping with both legs as our first attempt towards running. Using a dynamic model of HRP-2LR, hopping patterns are pre-calculated so that it follows the desired profiles of the total linear and angular momentum. For this purpose we used Resolved Momentum Control. Adding small modifications to negotiate the difference between the model and the real hardware, we successfully realized a steady hopping motion of 0.06 [s] flight phase and 0.5 [s] support phase. A hopping with forward velocity of 15 [mm/s] was also realized. Finally, a running pattern of 0.06 [s] flight and 0.3 [s] support phase was tested. HRP-2LR could successfully run with average speed of 0.16 [m/s].**

I. Introduction

Research on humanoid robots is currently one of the most exciting topics in the field of robotics and there exist many projects [1]–[5]. Most of them are focusing on biped walking as an important subject and have already demonstrated reliable dynamic biped walking. Watching those successful demonstrations, one can ask a natural question, "Can we build a humanoid that can run?"

We believe this is worthwhile as a technical challenge for the following reasons. First, studying robot running will add new functions of mobility to humanoid robots. For example, jumping over large obstacles or a crevasse in the ground might be realized by a derivative of the running control. Second, studying extreme situations will give us insights for improving the hardware itself. Current robots are too fragile to operate in any environment. Even when the robot operates at low speed, we must treat them carefully. We hope to overcome this fragility in the process of developing a running humanoid.

Running robots have been intensively studied by Raibert and his colleagues [6]. Their famous hopping robots driven by pneumatic and hydraulic actuators performed various actions including somersaults [7]. Using a similar control strategy, Hodgins simulated a running human in the computer graphics [8].

Ahmadi and Buehler studied running monopods from a standpoint of energy efficiency. Their ARL Monopod II [9] is an electrically powered running robot of 18 [kg] weight and could run at 1.25 [m/s] with a power expenditure of only 48 [W].

Recently, this hopping type of robot control has attracted many researchers interested in new applications such as space exploration [10]–[13].

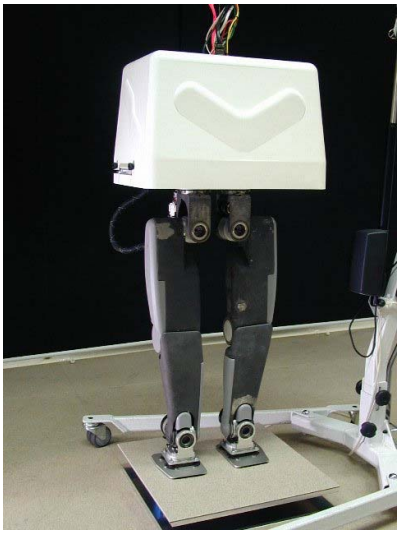

Fig. 1. Humanoid biped HRP-2LR

All of those robots have a spring mechanism to retrieve kinetic energy during running cycles. It is obvious that these springs help running but they might prevent the ordinary humanoid activities including walking, carrying objects and so on. Since our intention is to add a running function to a versatile humanoid robot, we started with a mechanism without springs. A similar approach is taken by Gienger et al. [1].

In our previous report [14], we investigated a running motion of an existing humanoid robot HRP-1 of 1.6 [m] height and 117 [kg] weight, which was developed in the Humanoid Robotics Project (HRP for short) of the Ministry of Economy, Trade and Industry of Japan. To generate a running pattern we proposed a method based on a simple inverted pendulum with some ad hoc modifications to absorb modeling error. From our simulation, it turned out that we require unrealizable 7 [kW] for some actuators of HRP-1 running at 2.9 [m/s].

In this paper, we introduce a newly developed biped HRP-2LR (Fig. 1) and its hopping experiment as the first attempt to realize a running biped. In Section II, we explain the hardware of HRP-2LR. A method to generate dynamic pattern is described in Section III. In Section IV, we show the experimental results of vertical hopping by playing back an off-line generated pattern, and introduce an adjustment to obtain accurate flight time. In Section V, we show the experimental

TABLE I

SPECIFICATIONS OF HRP-2LR

Size	6D.O.F/Leg(Hip:3 Knee:1 Ankle:2)	
	Upper leg length:	300 [mm]
	Lower leg length:	300 [mm]
	Ankle-sole height:	93 [mm]
	Length between hip joints:	120 [mm]
	Toe-heel length:	170 [mm]
Weight	Legs:8.6 [kg/leg]×2 [legs] =	17.2 [kg]
	Controller:	7.0 [kg]
	Body structure	6.8 [kg]
	Total:	31.0 [kg]

TABLE II

ACTUATORS AND HARMONIC DRIVE GEARS (HDG)

Joint		Actuator	Ratio of HDG
Hip	Yaw	20 [W]	1:160
	Roll	90 [W]	1:160
	Pitch	90 [W]	1:120
Knee	Pitch	150 [W]	1:100
Ankle	Pitch	90 [W]	1:160
	Roll	70 [W]	1:160

results of forward hopping and introduce an adjustment to obtain accurate travel distance. In Section VI, our first attempt to realize running is explained. We conclude this paper and address our future plan by Section VII.

II. HUMANOID BIPED HRP-2LR

HRP-2LR was originally developed as an "Advanced Leg Module" in HRP [15]. To make it as light as possible, we removed onboard batteries and the dummy weight which emulated the mass of arms, head and chest. Through this remodeling, the total weight was reduced from 58.2 [kg] to 31.0 [kg] and the height shortened from 1.41 [m] to 1.27 [m]. Detailed specifications of HRP-2LR and its actuators are shown in Tables I and II.

The body contains a 3-axes acceleration sensor, three gyro sensors, twelve servo drivers and a CPU board (Pentium III, 933 [MHz]). Each foot is equipped with a 6-axes force sensor and rubber bushing which protects the sensor and robot from the touchdown impact.

III. DYNAMIC PATTERN GENERATION

Our basic idea of hopping pattern generation is to calculate joint motions that produce the desired time profile of total linear momentum and angular momentum of a robot.

No matter how complex robot's structure or behavior becomes, we can determine the position of the total center of mass (CoM) $\tilde{\boldsymbol{c}}(3\times1)$, the linear momentum $\boldsymbol{P}(3\times1)$ and the angular momentum $\boldsymbol{L}(3\times1)$ for the total mechanism. Dividing the total linear momentum $\boldsymbol{P}$ by the total mass of the robot $\tilde{m}$, we obtain the CoM velocity.

$$\frac{d}{dt}\tilde{\boldsymbol{c}} = \frac{\boldsymbol{P}}{\tilde{m}} \tag{1}$$

Thus, we can control the CoM position by manipulating the linear momentum.

Considering this relationship, we proposed a method of control or pattern generation based on the total (linear and angular) momentum, and named this *Resolved Momentum Control* [16]. Following subsections review the outline of this method.

A. Momentum and joint velocities

We represent a biped robot as a mechanism of tree structure whose root is the base link (pelvis), a free-flying rigid body having 6 D.O.F (Degrees of Freedom) in space(Fig. 2). In this paper, we represent all vectors of position, velocity, angular velocity and related matrices in the world frame Σ_O fixed on the ground.

We define frame Σ_B at the center of the base link whose translational velocity and angular velocity are $\boldsymbol{v}_B(3\times1)$ and $\boldsymbol{\omega}_B(3\times1)$, respectively. In addition, we define the column vector $\dot{\boldsymbol{\theta}}_{leg_i}(6\times1)$ which contains joint velocities of each leg, $i=1$ for the right and $i=2$ for the left. The linear momentum $\boldsymbol{P}$ and the angular momentum $\boldsymbol{L}$ of the whole mechanism are given by

$$\begin{bmatrix}\boldsymbol{P}\\ \boldsymbol{L}\end{bmatrix} = \begin{bmatrix}\tilde{m}\boldsymbol{E} & -\tilde{m}\hat{\boldsymbol{r}}_{B\to\tilde{c}}\\ \boldsymbol{0} & \tilde{\boldsymbol{I}}\end{bmatrix}\begin{bmatrix}\boldsymbol{v}_B\\ \boldsymbol{\omega}_B\end{bmatrix} + \sum_{i=1}^{2}\begin{bmatrix}\boldsymbol{M}_{leg_i}\\ \boldsymbol{H}_{leg_i}\end{bmatrix}\dot{\boldsymbol{\theta}}_{leg_i}, \tag{2}$$

where $\boldsymbol{E}$ is the identity matrix of 3×3, $\boldsymbol{r}_{B\to\tilde{c}}(3\times1)$ is the vector from the base link to the CoM and $\tilde{\boldsymbol{I}}(3\times3)$ is the inertia matrix with respect to the CoM. $\boldsymbol{M}_{leg_i}(3\times6)$ and $\boldsymbol{H}_{leg_i}(3\times6)$ are the inertia matrices which indicate how the leg joint speeds affect to the linear momentum and the angular momentum respectively. These matrices can be calculated from physical parameters of the robot links and instantaneous configuration [16]. $\hat{}$ is an operator which translates a vector of 3×1 into a skew symmetric matrix of 3×3 which is equivalent to a cross product.

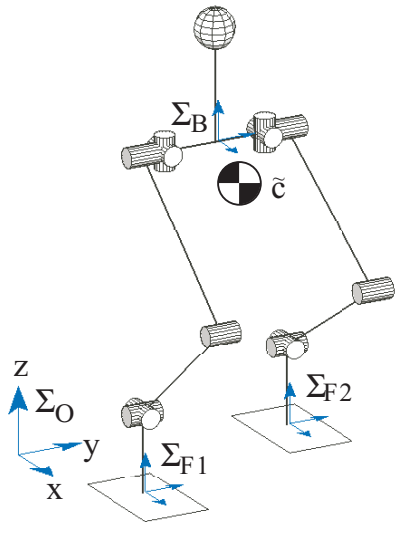

Fig. 2. Structure of HRP-2LR

B. Constraints of foot motion

Equation (2) calculates the total momentum of a biped with given configuration and joint velocities. However, when we specify the foot trajectory in the world frame, we need to consider the constraints that reduce the total D.O.F of the system. The foot velocities $(\boldsymbol{v}_{F_i}, \boldsymbol{\omega}_{F_i})$ for frame $\Sigma_{F_i} (i = 1, 2)$ are given by

$$\begin{bmatrix} \boldsymbol{v}_{F_i} \\ \boldsymbol{\omega}_{F_i} \end{bmatrix} = \begin{bmatrix} \boldsymbol{E} & -\hat{\boldsymbol{r}}_{B \to F_i} \\ \boldsymbol{0} & \boldsymbol{E} \end{bmatrix} \begin{bmatrix} \boldsymbol{v}_B \\ \boldsymbol{\omega}_B \end{bmatrix} + \boldsymbol{J}_{leg_i} \dot{\boldsymbol{\theta}}_{leg_i}, \quad (3)$$

where $\boldsymbol{J}_{leg_i} (6 \times 6)$ is the Jacobian matrix calculated from the leg configuration and $\boldsymbol{r}_{B \to F_i} (3 \times 1)$ is the position vector from the base link to the foot frame. If $\boldsymbol{J}_{leg_i} (i = 1, 2)$ are non singular, the velocities of the leg joint are given by

$$\dot{\boldsymbol{\theta}}_{leg_i} = \boldsymbol{J}^{-1}_{leg_i} \begin{bmatrix} \boldsymbol{v}_{F_i} \\ \boldsymbol{\omega}_{F_i} \end{bmatrix} - \boldsymbol{J}^{-1}_{leg_i} \begin{bmatrix} \boldsymbol{E} & -\hat{\boldsymbol{r}}_{B \to F_i} \\ \boldsymbol{0} & \boldsymbol{E} \end{bmatrix} \begin{bmatrix} \boldsymbol{v}_B \\ \boldsymbol{\omega}_B \end{bmatrix}. \quad (4)$$

By substituting (4) into (2), we obtain the momentum equation under the constraint as

$$\begin{bmatrix} \boldsymbol{P} \\ \boldsymbol{L} \end{bmatrix} = \begin{bmatrix} \boldsymbol{M}^*_B \\ \boldsymbol{H}^*_B \end{bmatrix} \boldsymbol{\xi}_B + \sum_{n=1}^{2} \begin{bmatrix} \boldsymbol{M}^*_{Fi} \\ \boldsymbol{H}^*_{Fi} \end{bmatrix} \boldsymbol{\xi}_{F_i}, \quad (5)$$

where

$$\begin{aligned} \boldsymbol{\xi}_B &\equiv [\boldsymbol{v}_B^T \quad \boldsymbol{\omega}_B^T]^T, \\ \boldsymbol{\xi}_{F_i} &\equiv [\boldsymbol{v}_{F_i}^T \quad \boldsymbol{\omega}_{F_i}^T]^T, \\ \begin{bmatrix} \boldsymbol{M}^*_B \\ \boldsymbol{H}^*_B \end{bmatrix} &\equiv \begin{bmatrix} \tilde{m}\boldsymbol{E} & -\tilde{m}\hat{\boldsymbol{r}}_{B \to \tilde{c}} \\ \boldsymbol{0} & \tilde{\boldsymbol{I}} \end{bmatrix} \\ &\quad - \sum_{n=1}^{2} \begin{bmatrix} \boldsymbol{M}^*_{Fi} \\ \boldsymbol{H}^*_{Fi} \end{bmatrix} \begin{bmatrix} \boldsymbol{E} & -\hat{\boldsymbol{r}}_{B \to F_i} \\ \boldsymbol{0} & \boldsymbol{E} \end{bmatrix} \end{aligned}$$

and

$$\begin{bmatrix} \boldsymbol{M}^*_{Fi} \\ \boldsymbol{H}^*_{Fi} \end{bmatrix} \equiv \begin{bmatrix} \boldsymbol{M}_{leg_i} \\ \boldsymbol{H}_{leg_i} \end{bmatrix} \boldsymbol{J}^{-1}_{leg_i}.$$

The second term in the right hand side of (5) indicates the extra momentum generated by specifying the foot speed.

C. Resolved Momentum Control

From (5) we can easily calculate the body velocity which realizes the reference total momentum $\boldsymbol{P}^{ref}$ and $\boldsymbol{L}^{ref}$ as

$$\boldsymbol{\xi}_B = \begin{bmatrix} \boldsymbol{M}^*_B \\ \boldsymbol{H}^*_B \end{bmatrix}^{-1} \left(\begin{bmatrix} \boldsymbol{P}^{ref} \\ \boldsymbol{L}^{ref} \end{bmatrix} - \sum_{n=1}^{2} \begin{bmatrix} \boldsymbol{M}^*_{Fi} \\ \boldsymbol{H}^*_{Fi} \end{bmatrix} \boldsymbol{\xi}^{ref}_{F_i} \right), \quad (6)$$

where $\boldsymbol{\xi}^{ref}_{F_i}$ is the reference velocity for each foot. This equation gives the Resolved Momentum Control for HRP-2LR. Although similar strategy have already proposed by Arikawa and Mita [17] to control a jumping robot, our method offers a systematic recipe for motion planning in 3D space.

IV. Vertical Hopping Experiment

As the first step toward a running, we examine a hopping motion. Our intention is to control flight phase which takes a vital role in running motion. Since the robot uses both feet equally, we can minimize a risk of mechanical damage at failure.

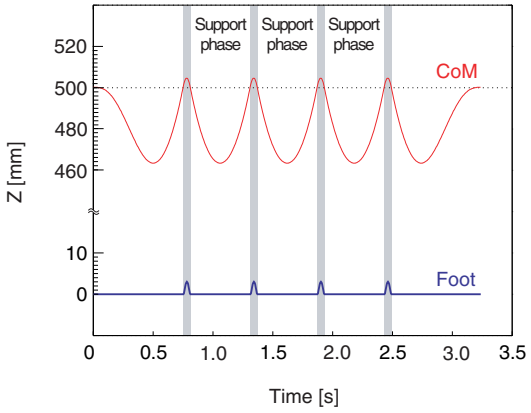

Fig. 3. CoM and foot trajectory for hopping

A. Reference motion

To design a vertical hopping motion, we must specify the vertical element of linear momentum P_z. With given flight time T_f and support time T_s the vertical element of linear momentum should be

$$\dot{P}^{ref}_z = \begin{cases} \frac{T_f}{T_s} \tilde{m} g & \text{(for support phase)} \\ -\tilde{m} g & \text{(for flight phase),} \end{cases} \quad (7)$$

where g is the gravity acceleration. In the case of vertical hopping, the other elements of the linear momentum should be zero i.e.

$$\dot{P}^{ref}_x = \dot{P}^{ref}_y = 0. \quad (8)$$

For the reference angular momentum we simply specified zero at all time i.e.

$$\dot{L}^{ref}_x = \dot{L}^{ref}_y = \dot{L}^{ref}_z = 0. \quad (9)$$

From these equations, we generated the momentum for $T_f = 0.06$ [s] and $T_s = 0.5$ [s]. The foot velocities $\boldsymbol{\xi}_{F_1}$ and $\boldsymbol{\xi}_{F_2}$ were generated by using a fourth order polynomial which realizes the liftoff and touchdown at specified time. Fig. 3 shows prescribed CoM and foot trajectory. The apex of foot trajectory is 3 [mm].

From reference momentum $\boldsymbol{P}^{ref}, \boldsymbol{L}^{ref}$ and reference foot velocity $\boldsymbol{\xi}^{ref}_{F_i}$, the resolved momentum control calculates the hopping pattern of HRP-2LR as a sequence of twelve joint angles for every 5 [ms].

B. Experiment and pattern improvement

By simply feeding the off-line calculated hopping motion as a reference for joint PD servo control of 1 [kHz], the robot could realize steady hopping motion. Fig. 4 shows the vertical floor reaction force measured by the force plate on the floor. The periods when the reaction force becomes about zero indicate the flight phase, and we can observe the robot made four successive hops. The maximum force of about 1000 [N] was generated at touchdown and it is within acceptable limits for the mechanical strength of HRP-2LR.

The average flight time of this experiment was 90 [ms], which was 1.5 times longer than the planned flight time of

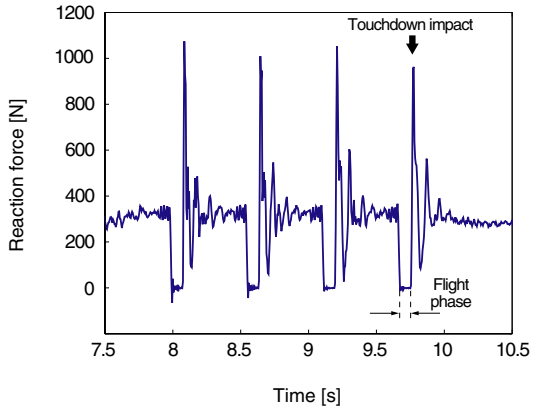

Fig. 4. Floor reaction force of vertical hopping

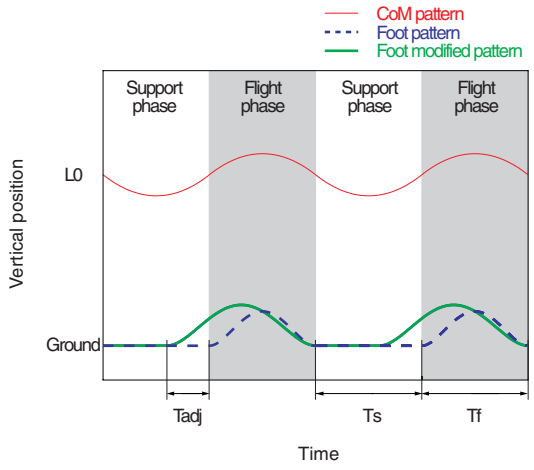

Fig. 5. Modification of liftoff time

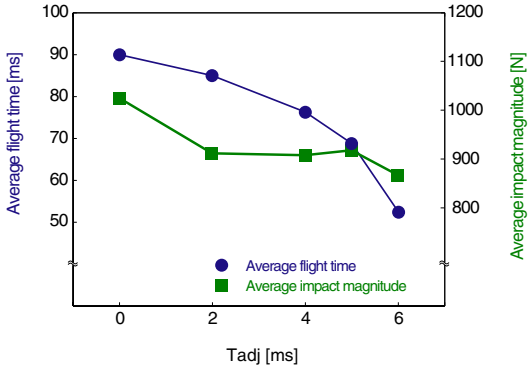

Fig. 6. Effect of liftoff modification T_{adj}

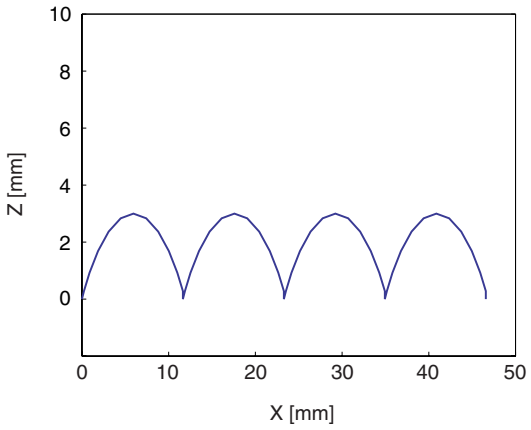

Fig. 7. Foot trajectory for forward hopping

60 [ms]. It is assumed that the structural compliance and servo compliance yielded such excessive flight time, since they were not considered in the reference pattern generation. To compensate this, we modified the start time of the foot lift as shown in Fig. 5. T_{adj} indicates the amount of quickened time of foot lift from the original pattern. By increasing this, we can expect to reduce the excessive body speed and flight time.

Fig. 6 shows the effect of this adjustment. As expected, we obtained a shorter flight time by increasing T_{adj}. The most accurate flight time was realized by giving $T_{adj} = 5$ [ms]. As a by-product of this adjustment, we obtained smaller touchdown impact which was desirable to protect the hardware.

V. Hopping with forward velocity

A. Reference motion

To let a robot go forward while hopping, we specified x element of the linear momentum as ,

$$\dot{P}_x^{ref} = \frac{\tilde{c}_x}{\tilde{c}_z}(\dot{P}_z^{ref} + \tilde{m}g). \quad (10)$$

By this equation, we can ensure a stable contact of feet during the support phase. The other elements of the momentum were kept unchanged from the vertical hopping. The horizontal foot trajectory was specified to proceed 12 [mm] at each hop as shown in Fig. 7.

B. Experiment and pattern improvement

A sequence of one hopping cycle is shown in Fig. 8. The second and the third picture from the left show the robot in the air (flight phase) although it is hard to recognize since the expected maximum distance between the soles and the ground was only 3 [mm]. We can confirm the steady hopping motion more clearly from the vertical floor reaction force shown in Fig. 9.

In the sequence of Fig. 8, the body posture was not kept upright during the hopping cycle. This is expected since the total angular momentum around the CoM was specified to be zero and the body had to rotate to maintain the angular momentum. Fig. 10 shows the pitch angular velocity of the body while hopping. The dashed line indicates the reference $\omega_{B_y}^{ref}$ and the solid line is the actual angular velocity ω_{B_y} measured by the onboard gyro sensor. The pitch angular velocity increases up to 2 [rad/s] (115 [deg/s]) in the flight

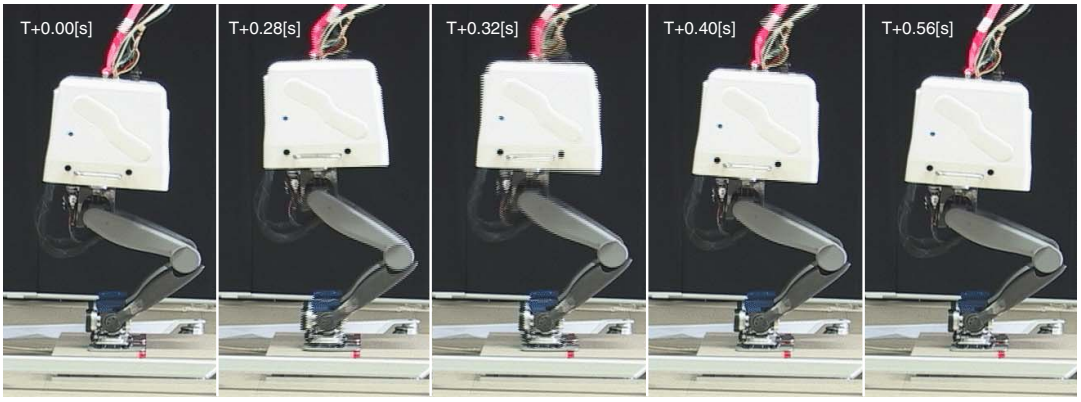

Fig. 8. Hopping with forward velocity: flight time: 0.06 [s], support time: 0.5 [s]

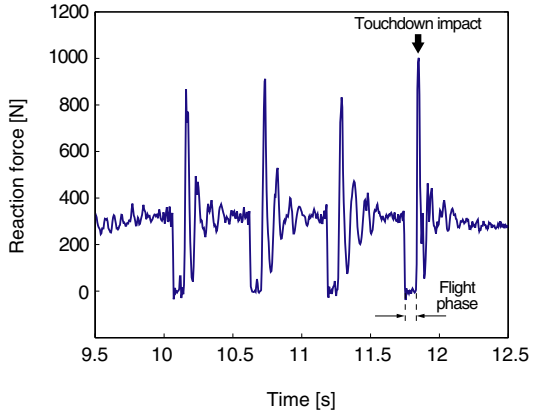

Fig. 9. Floor reaction force at forward hopping

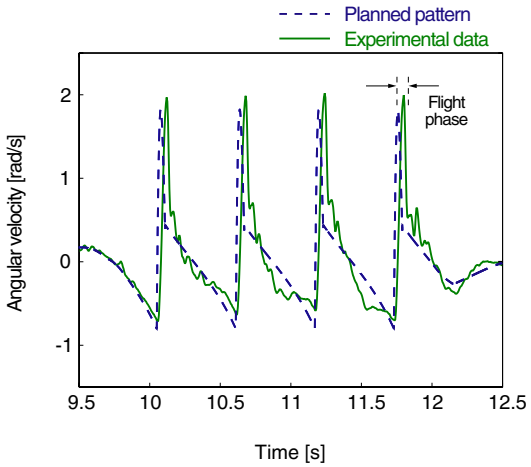

Fig. 10. Body angular velocity ω_{B_y} at forward hopping

phase to compensate the angular momentum generated by the legs moving towards the next support point.

In this experiment, the robot traveled only 40% of the distance expected by the reference pattern, partly because the robot was decelerated by the huge impact force at touchdown and could not recover the loss of momentum. To take this deceleration into account, we introduced discontinuous change of reference linear momentum. At the moment of expected touchdown, the reference was changed as

$$P_x^{ref+} = (1-\lambda)P_x^{ref-}, \tag{11}$$

where P_x^{ref-} and P_x^{ref+} are the reference momentum just before and just after touchdown respectively (Fig. 11). The parameter $\lambda \in [0, 1]$ determines the degree of the discontinuity. The reference linear momentum was calculated by (10) with the modification of (11) at each instant of the touchdown.

Fig. 12 shows the travel distance against λ. By giving proper parameter, the travel distance was increased up to 33 [mm]. The average speed at the best condition was 15 [mm/s].

Fig. 13 shows the close up of one "best" hop with travel distance of 8 [mm].

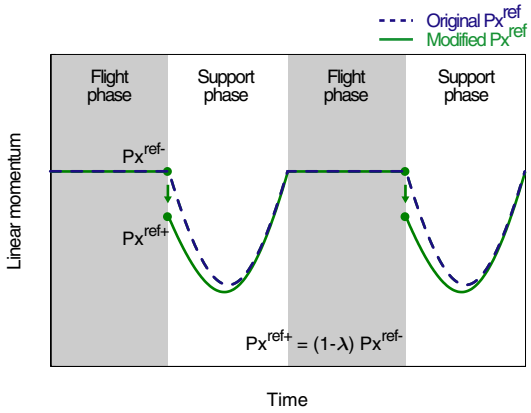

Fig. 11. Modifying forward linear momentum

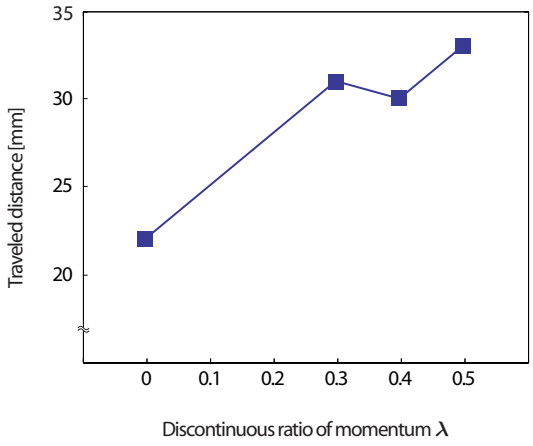

Fig. 12. Effects of the modification of reference momentum

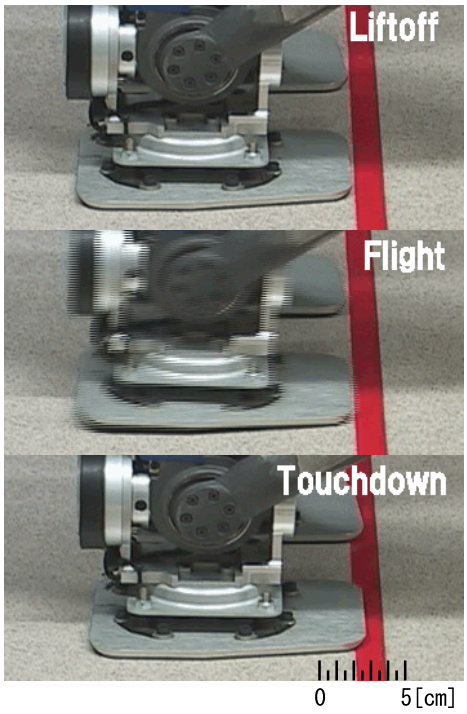

Fig. 13. Close-up of one forward hop

VI. Running Experiment

On December 18th, 2003, Sony Corporation announced that they created the world's first running humanoid robot [18]. Their robot QRIO is a self-contained 38 D.O.F humanoid, 580 [mm] height, 7 [kg] weight. QRIO demonstrated running with 14 [m/min] (0.23 [m/s]) whose flight phase is approx. 20[ms] [19]. Although the technical detail of their running control has not been well disclosed yet, it seems like they took a similar approach to us (no springs in the legs and running with short flight time).

Fig. 14 shows our first running experiment of HRP-2LR. The running pattern was created by the method of Section III,

TABLE III

Running Pattern and Result

Planned	Support time T_s:	0.3 [s]
	Flight time T_f:	0.06 [s]
	Travel distance:	0.81 [m]
	Average speed:	0.25 [m/s]
	Maximum foot height:	0.025 [m]
	Steps:	9 [step]
Result	Traveled distance:	0.55 [m]
	Average speed:	0.16 [m/s]

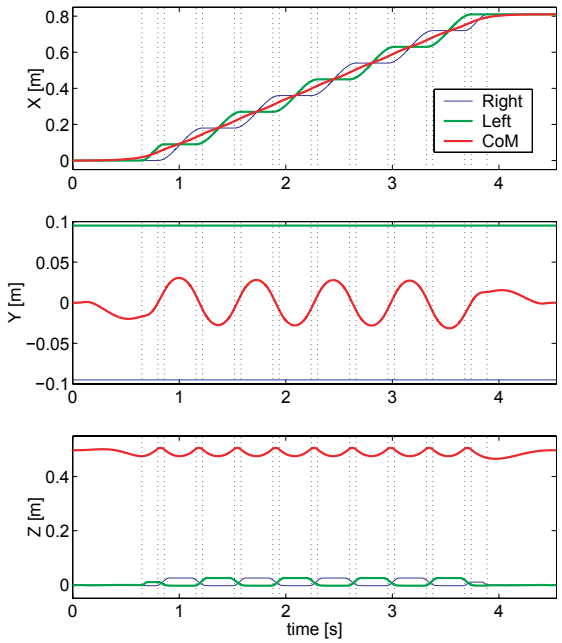

Fig. 15. CoM and foot trajectory for running

IV and V with additional modifications. The parameters of designed running pattern are listed in Table III. To realize a stable running, we developed a software module named *running stabilizer* which slightly changes the planned pattern using the gyros, the accelerometers and the foot force sensors. The running stabilizer works to keep the posture error and the speed error within acceptable level against the disturbance. The details of running pattern generation and the running stabilizer will appear in our next report.

Thanks to the well designed running pattern and the running stabilizer, HRP-2LR could successfully run with average speed of 0.16 [m/s]. The realized speed was 64% of planned value (0.25 [m/s]), due to slips between the robot soles and the ground. The running cycle, however, was well controlled as planned. We can confirm this by watching the vertical forces measured at the robot feet (Fig. 16).

VII. Conclusions

In this paper, we introduced biped robot HRP-2LR which was developed to realize running motion. Based on the parameter of HRP-2LR, hopping patterns were pre-calculated so that it follows the desired profiles of the total linear and

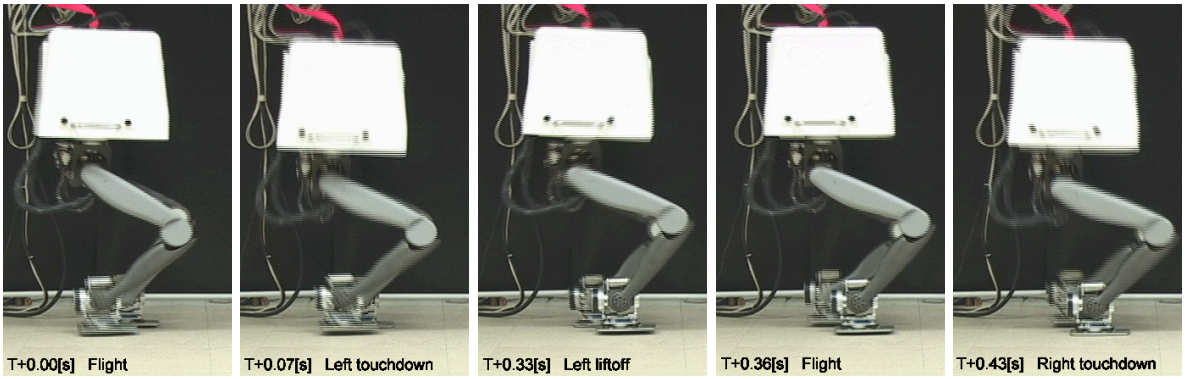

Fig. 14. Running experiment of HRP-2LR. The robot is running from left to right with average speed of 0.16 [m/s].

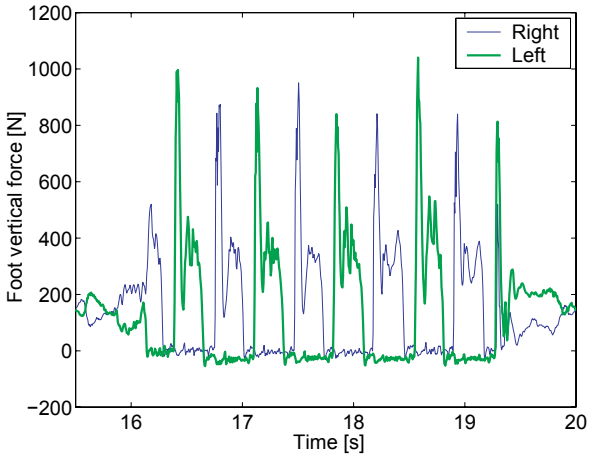

Fig. 16. Vertical foot force at running experiment

angular momentum. For this purpose we used the Resolved Momentum Control. Adding small modifications to negotiate the difference between the model and the hardware, we successfully realized a steady hopping motion of 0.06 [s] flight phase and 0.5 [s] support phase. A hopping with forward velocity of 15 [mm/s] was also realized.

In the hopping experiments of this paper, we deliberately used slow speed because the robot lost its stability under the higher speed due to the mechanical compliance. To cope with this problem, we developed a stabilization control using gyros, acceleration sensors and force sensors. Using the running stabilizer, HRP-2LR could successfully run with 0.16 [m/s]. This running pattern generation and its control will be described in our next report.

ACKNOWLEDGMENT

We thank people of Kawada Industries, Inc. especially Jiro Sakurai, Toshikazu Kawasaki and Takakatsu Isozumi for their professional technical support. We also thank Hirohisa Hirukawa, Fumio Kanehiro, Kiyoshi Fujiwara, Kensuke Harada and Hajime Saito of Humanoid Research Group, AIST for their excellent advice.

REFERENCES

[1] Gienger, M., et.al, "Toward the Design of a Biped Jogging Robot," Proc. of the 2001 ICRA, pp.4140–4145, 2001.
[2] Hirai, K., Hirose, M., Haikawa, Y. and Takenaka, T., "The Development of Honda Humanoid Robot," Proc. of the 1998 ICRA, pp.1321–1326, 1998.
[3] Inoue, H., Tachi, S., Nakamura, Y., Hirai, K., et.al, "Overview of Humanoid Robotics Project of METI," Proc. Int. Symp. Robotics, pp.1478–1482, 2001.
[4] Nishiwaki, K., Sugihara, T., Kagami, S., Kanehiro, F., Inaba, M., and Inoue, H., "Design and Development of Research Platform for Perception-Action Integration in Humanoid Robot: H6," Proc. Int. Conference on Intelligent Robots and Systems, pp.1559–1564, 2000.
[5] Yamaguchi, J., Soga, E., Inoue, S. and Takanishi, A., "Development of a Bipedal Humanoid Robot – Control Method of Whole Body Cooperative Dynamic Biped Walking –," Proc. of the 1999 ICRA, pp.368–374, 1999.
[6] Raibert, M., *Legged Robots that Balance*, Cambridge, MA, MIT Press, 1986.
[7] Playter, Robert R. and Raibert, Marc H., "Control of a Biped Somersault in 3D," Proc. of IFToMM-jc International Symposium on Theory of Machines and Mechanisms (in Nagoya, Japan), pp.669–674, 1992.
[8] Hodgins, J. K.,"Three-Dimensional Human Running," Proc. of the 1996 ICRA, pp.3271-3277, 1996.
[9] Ahmadi, M. and Buehler, M., "The ARL Monopod II Running Robot: Control and Energetics," Proc. of the 1999 ICRA, pp.1689-1694, 1999.
[10] Hale, E., Schara, N., Burdick, J. and Fiorini, P., "A Minimally Actuated Hopping Rover for Exploration of Celestial Bodies," Proc. of the 2000 ICRA, pp.420–427, 2000.
[11] Shimoda, S., Wingart, A. and Takahashi, K., "Microgravity Hopping Robot with Controlled Hopping and Landing Capability," Proc. of the 2003 ICRA, pp.2571–2576, 2003.
[12] Harbick, K. and Sukhatme, G. S., "Controlling Hopping Height of a Pneumatic Monopod," Proc. of the 2002 ICRA, pp.3998–4003, 2002.
[13] Mombaur, K. D., Longman, R. W., Bock, H. G. and Schlöder, J. P., "Stable One-Legged Hopping Without Feedback and With a Point Foot," Proc. of the 2002 ICRA, pp.3978–3983, 2002.
[14] Kajita, S. et al.,"Running Pattern Generation for a Humanoid Robot," Proc. of the 2002 ICRA, pp.2755–2761, 2002.
[15] Kaneko, K. et al.,"Design of Advanced Leg Module for Humanoid Robotics Project of METI," Proc. of the 2002 ICRA, pp.38–45, 2002.
[16] Kajita, S., Kanehiro, F., Kaneko, K., Fujiwara, K., Harada, K., Yokoi, K. and Hirukawa, H., "Resolved Momentum Control: Humanoid Motion Planning based on the Linear and Angular Momentum," Proc. of the 2003 IROS, pp.1644–1650, 2003.
[17] Arikawa, K. and Mita, T, "Design of Multi-DOF Jumping Robot," Proc. of the 2002 ICRA, pp.3992–3997, 2002.
[18] http://www.sony.net/SonyInfo/News/Press/200312/03-060E
[19] http://pc.watch.impress.co.jp/docs/2003/1218/sony.htm (in Japanese)